

## Original Article



# Inhibition of Indoleamine 2,3-Dioxygenase Enhances the Therapeutic Efficacy of Immunogenic Chemotherapeutics in Breast Cancer

Jian Gao <sup>1,2</sup>, Fusheng Deng <sup>2</sup>, Weidong Jia <sup>3</sup>

<sup>1</sup>Department of Clinical Medicine, Clinical Medical College of Shandong University, Jinan, China

<sup>2</sup>Department of General Surgery, the First Affiliated Hospital of University of Science and Technology of China, Division of Life Sciences and Medicine, University of Science and Technology of China, Hefei, China

<sup>3</sup>Department of Hepatic Surgery, the First Affiliated Hospital of University of Science and Technology of China, Division of Life Sciences and Medicine, University of Science and Technology of China, Hefei, China

## OPEN ACCESS

Received: Dec 11, 2018

Accepted: Apr 12, 2019

### Correspondence to

Weidong Jia

Department of Hepatic Surgery, the First Affiliated Hospital of University of Science and Technology of China, Division of Life Sciences and Medicine, University of Science and Technology of China, Hefei 230001, China.  
E-mail: wdjia2018@sina.com

© 2019 Korean Breast Cancer Society

This is an Open Access article distributed under the terms of the Creative Commons Attribution Non-Commercial License (<https://creativecommons.org/licenses/by-nc/4.0/>) which permits unrestricted non-commercial use, distribution, and reproduction in any medium, provided the original work is properly cited.

### ORCID iDs

Jian Gao

<https://orcid.org/0000-0003-4746-0824>

Fusheng Deng

<https://orcid.org/0000-0003-1589-162X>

Weidong Jia

<https://orcid.org/0000-0002-1056-0584>

### Conflict of Interest

The authors declare that they have no competing interests.

### Author Contributions

Conceptualization: Gao J; Data curation: Gao J, Deng F; Formal analysis: Deng F; Writing - original draft: Jia W; Writing - review & editing: Jia W.

## ABSTRACT

**Purpose:** Breast cancer has become a major public health threat in the current society. Anthracycline doxorubicin (DOX) is a widely used drug in breast cancer chemotherapy. We aimed to investigate the immunogenic death of breast tumor cells caused by DOX, and detect the effects of combination of DOX and a small molecule inhibitor in tumor engrafted mouse model.

**Methods:** We used 4T1 breast cancer cells to examine the anthracycline DOX-mediated immunogenic death of breast tumor cells by assessing the calreticulin exposure and adenosine triphosphate and high mobility group box 1 release. Using 4T1 tumor cell-engrafted mouse model, we also detected the expression of indoleamine 2,3-dioxygenase (IDO) in tumor tissues after DOX treatment and further explored whether the specific small molecule IDO1 inhibitor NLG919 combined with DOX, can exhibit better therapeutic effects on breast cancer.

**Results:** DOX induced immunogenic cell death of murine breast cancer cells 4T1 as well as the upregulation of IDO1. We also found that treatment with NLG919 enhanced kynurenine inhibition in a dose-dependent manner. IDO1 inhibition reversed CD8<sup>+</sup> T cell suppression mediated by IDO-expressing 4T1 murine breast cancer cells. Compared to the single agent or control, combination of DOX and NLG919 significantly inhibited the tumor growth, indicating that the 2 drugs exhibit synergistic effect. The combination therapy also increased the expression of transforming growth factor- $\beta$ , while lowering the expressions of interleukin-12p70 and interferon- $\gamma$ .

**Conclusion:** Compared to single agent therapy, combination of NLG919 with DOX demonstrated better therapeutic effects in 4T1 murine breast tumor model. IDO inhibition by NLG919 enhanced the therapeutic efficacy of DOX in breast cancer, achieving synergistic effect.

**Keywords:** Breast neoplasms; Chemotherapy; Doxorubicin; Indoleamine 2,3-dioxygenase

## INTRODUCTION

Breast cancer has become a major public health threat in the current society. The global incidence of breast cancer has been rising since the late 1970s. The annual cancer report

released by the American Cancer Society shows that the incidence of breast cancer ranks first among female malignant tumors, accounting for 30% of all types of cancers [1,2]. At present, breast cancer treatment methods mainly include surgery, radiotherapy, chemotherapy, hormone therapy, and targeted therapy. For advanced and metastatic breast cancer (MBC), systemic chemotherapy is one of the most important comprehensive treatments, and more than 80% of breast cancer patients need chemotherapy-assisted treatment after surgery [3]. Anthracyclines play an important role in breast cancer chemotherapy, which are widely used in single-agent or combination therapy for advanced breast cancer, or adjuvant chemotherapy following breast tumor surgery [4].

Recent studies have found that some anthracyclines, such as doxorubicin (DOX), not only induce tumor cell apoptosis, but also cause immunogenic cell death (ICD) [5]. When immunogenic death occurs, tumor cells release 3 types of signals: 1) The exposure of calreticulin (CRT) on the cell surface, stimulating the phagocytosis of tumor cells by dendritic cells (DCs); 2) The release of adenosine triphosphate (ATP), recruiting DCs into tumor foci; and 3) The release of high mobility group box 1 (HMGB1) that promotes the binding of DCs with dying tumor cells, activating tumor specific cytotoxic T lymphocytes [6]. Although chemotherapeutic drugs, such as DOX, that induce immunogenic death in cells can activate the body's anti-tumor immune response to a certain extent in clinical practice, the treatment using such drugs is not satisfactory, and one of the possible reasons could be the presence of complex immunosuppressive signaling pathways in the tumor microenvironment [7]. Studies have shown that combined immunogenic chemotherapy drugs and antibody drugs or small molecule drugs that reverse the tumor immunosuppressive microenvironment are expected to achieve better tumor treatment effects [8]. A large number of studies have shown that indoleamine 2,3-dioxygenase 1 (IDO1) can catalyze the metabolism of tryptophan (Trp) in the tumor microenvironment, which, in turn, interferes with the function of cytotoxic sputum cells, leads to immunosuppression [9].

In this study, we aimed to investigate the anthracycline DOX-mediated immunogenic death of breast tumor cells by assessing the CRT exposure and ATP and HMGB1 release in 4T1 breast cancer cells, which mimic stage IV human breast cancer cells. Using 4T1 tumor cell engrafted mouse model, we also detected the expression of IDO in tumor tissues after DOX treatment and further explored whether the combination of DOX and the specific small molecule IDO1 inhibitor NLG919, which is being investigated for the treatment of immunosuppression associated with cancer, could achieve better therapeutic effects in breast cancer.

## METHODS

### Cell lines and animals

Mouse mammary tumor cell line 4T1 was obtained from Shanghai Liangtai Biotechnology (Shanghai, China). Cells were cultured in RPMI 1640 medium (Thermo Fisher Scientific, New York, USA), supplemented with 10% heat-inactivated fetal bovine serum, 10 mM HEPES, 10 U/mL penicillin, and 10 mg/mL streptomycin, at 37°C in humidified cell incubator under 5% CO<sub>2</sub>. All animal studies were approved by the Institutional Animal Care and Use Committee of the First Affiliated Hospital of University of Science and Technology of China (#AHM20170842J). Female BALB/c mice (6–8 weeks old) were housed in animal facility with controlled temperature and humidity in a 12/12 (light/dark) schedule. Food and water were available to the mouse ad libitum.

### Drug treatment

DOX hydrochloride was purchased from Sigma-Aldrich Chemical Co. (St. Louis, USA). Cells were seeded into 12-well plates at a concentration of  $1 \times 10^5$  cells/well, and incubated for 24 hours until they reached 50% confluence. While considering the half-maximal inhibitory concentration of DOX determined in our study (**Supplementary Figure 1**) and previous report [10], cells were incubated with DOX at concentrations of 0.1  $\mu$ M, 0.25  $\mu$ M, and 0.5  $\mu$ M for additional 24 hour at 37°C in a CO<sub>2</sub> incubator. Cells in the control group were incubated with HEPES buffer (pH 7.4) for the same duration. All the treated cells were subjected to the biochemical assays described in following sections.

### Flow cytometric analysis of CRT on the cell surface

After the drug treatment, 4T1 cells were harvested and washed with  $1 \times$  phosphate buffer saline (PBS). Then, the cells were fixed in 0.25% paraformaldehyde for 5 minutes. Pre-chilled PBS was used to wash fixed cells twice, and the cells were incubated with anti-CRT antibody (Novus Biologicals, Littleton, USA) in Cell Staining Buffer (Biolegend, Dedham, USA) for 30 minutes. Control cells were incubated with immunoglobulin G antibody. The fluorescence intensity of stained cells was gated on propidium iodide-negative cells, and cell surface CRT was analyzed by FACScan (Becton-Dickinson, Franklin Lakes, USA).

### Detection of HMGB1 and ATP releases

After 48 hours of drug treatment, the culture supernatant of 4T1 cells was collected. The HMGB1 was quantified using Western Blot. Equal amount of bovine serum albumin was used as a loading control. ATP level in the collected supernatant was detected using chemiluminescent ATP Determination Kit (Thermo Fisher Scientific, Waltham, USA), according to the manufacturer's protocol. In brief, a standard curve was created using ATP standard solutions. Samples at the same volume were added into reaction solution containing D-luciferin, dithiothreitol, and firefly luciferase. The amount of ATP was then calculated using the luminescence intensity based on a standard luminescence curve.

### Mouse vaccination approach

Briefly, dying 4T1 cells treated with DOX were injected into the right flank of mice in 2 rounds at 7 days interval. Fourteen days after the first injection, the mice were administered with either normal 4T1 cell suspensions or DOX-treated 4T1 cells ( $1 \times 10^6$  cells) in the contralateral flank. Two weeks later, the number of mice without tumor on contralateral side was counted.

### In vivo DOX treatment and tumor measurement

To compare the inhibition of tumor growth by DOX, mouse breast tumor model was established by injecting normal 4T1 cells as above described, and DOX was injected into them at the dose of 5.0 mg/kg for 5 times at intervals of 3 days each, when the tumor volume reach about 50 mm<sup>3</sup>. Tumor volume was measured after every 4 days using an electronic caliper, and the mean tumor volumes (mm<sup>3</sup>) of the DOX and control groups were used to plot tumor growth curves.

### Quantitative real-time polymerase chain reaction (qRT-PCR)

qRT-PCR was performed to detect the relative messenger RNA (mRNA) expression of cytotoxic T-lymphocyte-associated protein 4 (CTLA-4), programmed cell death 1 (PD-1), PD-ligand 1 (PD-L1), IDO1, cerebrospinal fluid 1 (CSF-1), and chemokine (C-C motif) ligand 2 (CCL2) using primers obtained from TaKaRa (Takara Biotechnology, Dalian, China) on an ABI Prism 7000 Sequence Detection System (Perkin-Elmer Applied Biosystems, Foster

City, USA). The expression level of the housekeeping gene glyceraldehyde 3-phosphate dehydrogenase was used as an internal control. The expression levels of these genes in the control and DOX-treated groups were compared.

### Detection of IDO1 level by western blotting and immunohistochemistry (IHC)

The protein expression level of IDO1 was assessed by western blotting. Briefly, anti-IDO1 monoclonal antibody was incubated with the protein transferred to the polyvinylidene fluoride membrane, and  $\beta$ -actin was used as the loading control. For IHC, mouse anti-IDO1 monoclonal antibody (Abcam, Cambridge, USA) was used as the primary antibody to incubate with tissue sections at 4°C. Tissue sections were then incubated with the anti-mouse secondary antibody, followed by further incubation with the streptavidin-horseradish peroxidase complex. Tissue sections were lightly counterstained with hematoxylin and visualized using diaminobenzidine as a chromogen. Positive staining cells were captured under a microscope (Olympus, Tokyo, Japan) with magnification of 400 $\times$  to calculate the immunohistochemical signals.

### Knockdown of IDO1 in 4T1 cells

Short hairpin RNAs (shRNAs) targeting IDO1 (shIDO1#1, shIDO1#2, and shIDO1#3) and non-target control (shNC) were purchased from Shanghai Genepharma Inc. (Shanghai, China), and transfected to 4T1 cells. Transfected cells were selected by the IDO1 expression level identified by western blotting, and the cells with stable transduction were used for breast tumor models as described earlier.

### Application of IDO1-specific inhibitor, NLG919

The inhibitory activity of NLG919, a highly selective inhibitor of IDO-1, was detected in 4T1 cell-based kynurenine (Kyn) assay, as previously described [11]. Specifically, 4T1 cells were treated with interferon (IFN)- $\gamma$  along with NLG919 at 0.1, 0.25, 0.5, 1.0, 2.5, 5.0, and 10  $\mu$ M, and Kyn in the cell culture supernatants was detected using high performance liquid chromatography mass spectrometry (HPLC-MS/MS).

The lymphocytes were isolated from BALB/c mouse spleen and stained with CellTrace™ CFSE dye (ThermoFisher Scientific). The 4T1 cells were stimulated with IFN- $\gamma$ , and added to the lymphocyte culture in the 96-well plates at concentrations of  $1 \times 10^5$  and  $5 \times 10^5$  cells per well, respectively. Then, 100 ng/mL anti-CD3 antibody (eBioscience, Thermo Fisher Scientific) and 10 ng/mL human recombinant interleukin (IL)-2 (R&D Systems, Shanghai, China) were added to the co-cultured cells. Three days later, CD8<sup>+</sup> T cell proliferation was detected by flow cytometry analysis. The 4T1 cells without spleen lymphocytes were used as a positive control.

### In vivo application of DOX and NLG919 combination

BALB/c mice bearing 4T1 tumors of ~50 mm<sup>3</sup> volume were administered vehicle control, DOX, NLG919, or a combination of DOX and NLG919 after every 3 days for 5 times; the administration dosage of DOX and NLG919 were 5.0 mg/kg (i.v.) and 20 mg/kg (orally), respectively. The tumor volume in each mouse group was measured as described earlier after every 3 days up to 21 days. The Kyn (nM)/Trp ( $\mu$ M) ratios in the tumor homogenates and plasma of mice in each group were assessed. Then, the tumor tissues were subjected to the hematoxylin and eosin stain (H&E) and proliferating cell nuclear antigen (PCNA) staining and analyzed by IHC.

### Mature DC analysis by flow cytometry analysis

Breast tumor tissues were digested using 2 mg/mL collagenase A (Roche, Indianapolis, USA) and 170 U/mL DNase I (Sigma-Aldrich Chemical Co.), and single-cell suspensions were prepared from the homogenates of tumor tissues. Cell samples were then stained with antibodies against CD45, CD11b<sup>+</sup>, CD11c<sup>+</sup>, CD80, and CD86. CD80<sup>+</sup> CD86<sup>+</sup> cells were denoted as mature DCs. In addition, CD8<sup>+</sup> T cells among the CD45<sup>+</sup> tumor infiltrating lymphocytes (TILs) in the tumor tissues were also analyzed.

### Cytokines determination by enzyme-linked immunosorbent assay (ELISA)

According to the manufacturer's protocol, ELISA was used to quantify levels of following cytokines in supernatants of the tumor tissues homogenates: transforming growth factor (TGF)- $\beta$ , IL-12p70 (eBioscience/Biosciences), and IFN- $\gamma$  (R&D systems). At least 3 independent experiments were conducted in each assay.

### Statistical analysis

SPSS software 13.0 (SPSS Inc., Chicago, USA) was used for statistical analysis throughout the study. The results were presented as mean  $\pm$  standard deviation. Statistical analysis was performed by 1- or 2-way analysis of variance. The differences between the DOX and control groups were evaluated by an independent sample *t*-test. The significance level was set at  $p < 0.05$ .

## RESULTS

### DOX induces ICD of murine breast cancer cells 4T1

In response to treatment with different concentrations of DOX, 4T1 cells underwent ICD, indicated by the pre-apoptotic translocation of CRT. As shown in **Figure 1A and B**, the percentage of CRT-positive cells among propidium iodide-negative cells increased after DOX treatment in a dose-dependent manner. In addition, the release of HMGB1 into the 4T1 cell culture medium was examined by western blot, and we found higher levels of soluble HMGB1 in the cells treated with higher doses of DOX (**Figure 1C**,  $p < 0.05$ ). Further, our results demonstrated that the ATP release also increased with increase in the doses of DOX in different cell groups (**Figure 1D**,  $p < 0.05$ ).

To investigate the *in vivo* effects of DOX on breast tumor, we injected DOX-treated 4T1 cells twice to one flank of mice every week, and then, injected normal 4T1 cells on the contralateral side of mice (**Figure 1E**). Two weeks later, we counted the number of mice without tumor on contralateral side, and the results showed that 5 out of 6 mice had no tumor for the 0.5  $\mu$ M DOX group, while all mice developed tumor on the contralateral side in the control group (**Figure 1F**), indicating the successful tumor growth inhibition by the immune interference of DOX.

### DOX treatment induces upregulation of IDO1 and IDO1 impairs the therapeutic efficacy of DOX

Using the 4T1 breast tumor engraft model, we observed less severe progression of tumor burden in the DOX-treated mice than the control mice (**Figure 2A**). RT-PCR results revealed that the mRNA expressions of PD-L1, IDO1, CSF-1, and CCL2 were upregulated in the DOX-treated mice, whereas the expression of CTLA-4 and PD-1 in the DOX-treated mice did not differ from that in the control mice. Among all detected genes, the relative expression level of the IDO1 gene demonstrated the largest difference between DOX and control groups

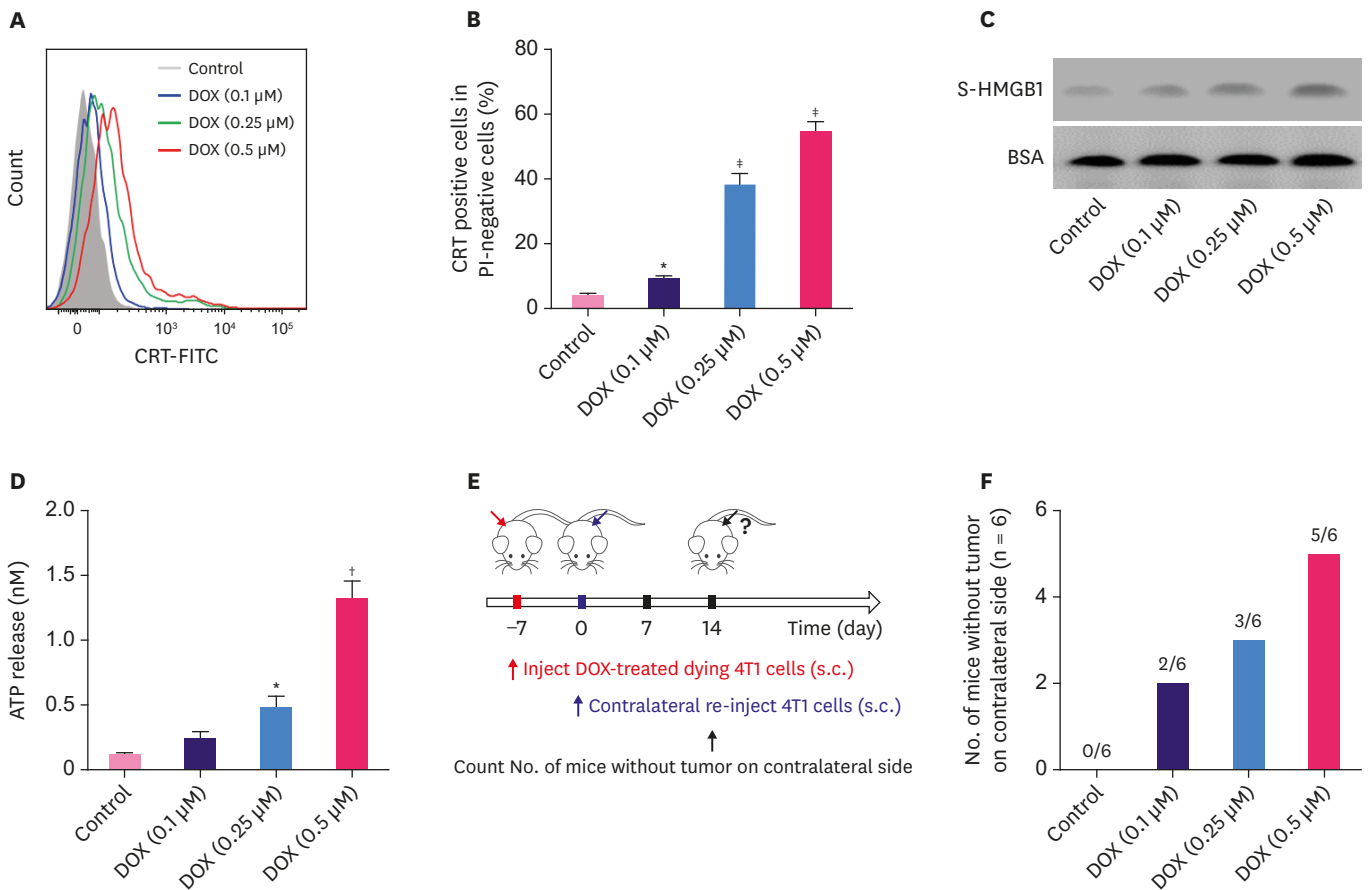


**Figure 1.** DOX induces immunogenic cell death of murine breast cancer cells 4T1. (A) The surface exposure of CRT was determined by flow cytometry among viable (propidium iodide-negative) cells after treatment with different concentrations of DOX for 24 hours. DOX-treated cells were stained with propidium iodide and FITC-labeled anti-CRT antibodies according to the manufacturer's instructions. (B) The percentage of CRT-positive cells in PI-negative cells was quantified based on the results of flow cytometry. (C) S-HMGB1 of 4T1 cells treated with different concentrations of DOX was measured by western blotting, and BSA was used as the loading control. (D) Level of released ATP was determined by a chemiluminescent ATP Determination Kit. (E) Animal vaccination, using 2 rounds of s.c. injection of DOX-treated dying 4T1 cells at 7 days apart, followed by s.c. injection of live cells on the contralateral side. Two weeks later, the number of mice without tumor on contralateral side was counted. Successful tumor growth inhibition at the challenge site is suggestive of immune interference. (F) The number of mice without visible tumor on contralateral side 2 weeks post second injection. Data represent means  $\pm$  standard deviation.

DOX = doxorubicin; ATP = adenosine triphosphate; BSA = bovine serum albumin; DOX = doxorubicin; CRT = calreticulin; FITC = fluorescein isothiocyanate; PI = propidium iodide; SD = standard deviation; S-HMGB1 = supernatant high mobility group box 1; s.c. = subcutaneous.

\* $p < 0.05$ ; † $p < 0.01$ ; ‡ $p < 0.001$  (versus control group).

(**Figure 2B**,  $p < 0.001$ ). Similar upregulated expression of IDO1 was also validated by western blot (**Figure 2C**). In addition, we found that the DOX expression in the H&E stained tumor sections in DOX-treated mice was significantly higher than that in the control mice (**Figure 2D**).

To validate the activity of IDO1 during tumor growth, we used shRNA to knockdown the expression of IDO1 in 4T1 cells. Among 3 candidate shRNAs including shIDO1#1, shIDO1#2, and shIDO1#3, shIDO1#1 significantly inhibited the expression of IDO1 in 4T1 cells and DOX-treated cells (**Figure 2E** and **Supplementary Figure 2A**). In addition, upregulation of IDO1 in 4T1 cells (transfected with IDO1 plasmid) caused resistance to DOX (**Supplementary Figure 2B**). Furthermore, we injected shIDO1#1 transfected 4T1 (4T1-shIDO1#1) cells into BALB/c mice. In comparison with the 4T1-shNC cells, 4T1-shIDO1#1-bearing mice showed significantly slower tumor growth. Strikingly, the co-administration of 4T1-shIDO1#1 and DOX exhibited brilliant inhibition of tumor growth in the engrafted model (**Figure 2F**,  $p < 0.05$ ).



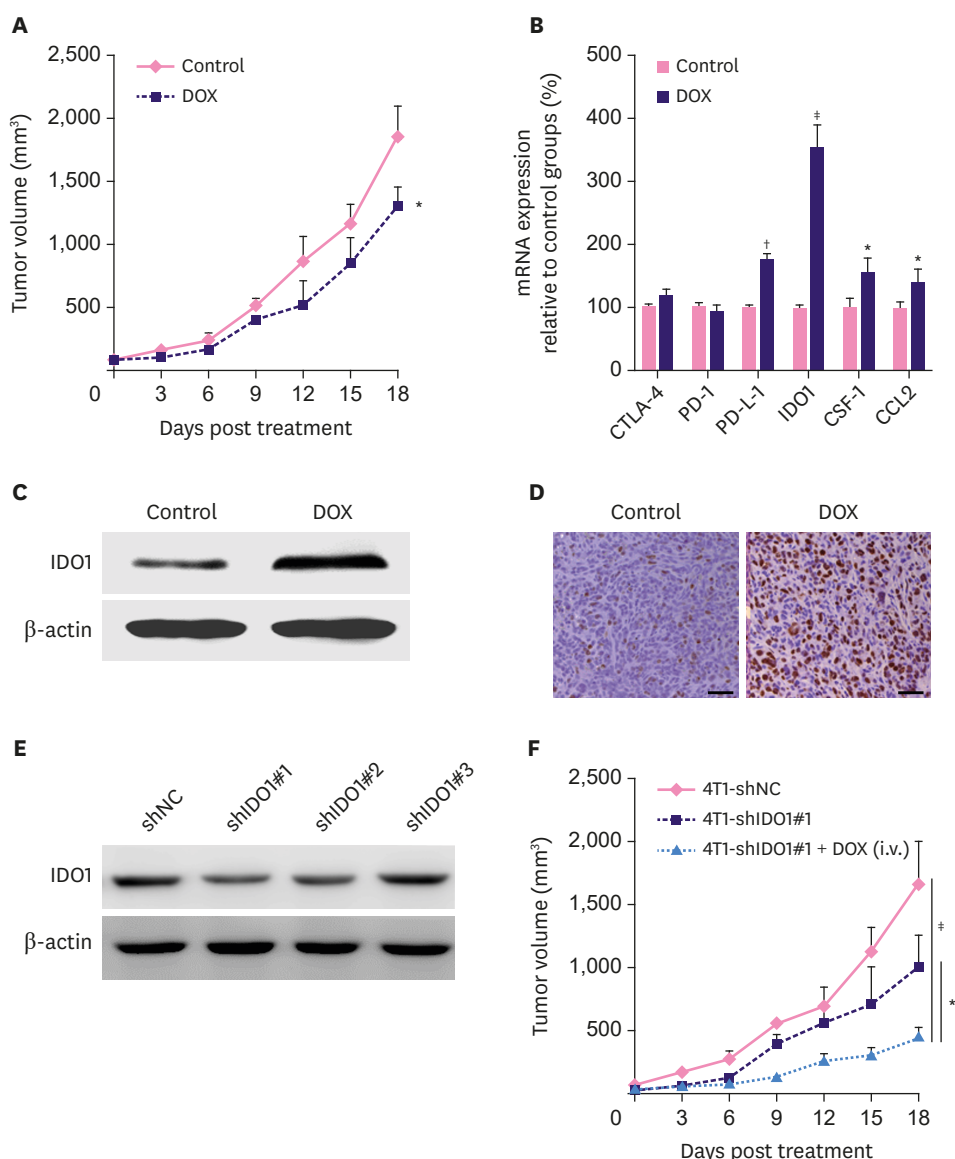


**Figure 2.** DOX treatment induces upregulation of IDO1 and IDO1 impairs the therapeutic efficacy of DOX. (A) Slight inhibition of tumor growth by DOX in 4T1 tumor-bearing BALB/c mice (n = 6). DOX was i.v. injected at the dosage of 5.0 mg/kg for 5 times after every 3 days. (B) The mRNA expressions of CTLA-4, PD-1, PD-L1, IDO1, CSF-1, and CCL2 examined by real time polymerase chain reaction. The mRNA levels of these genes were normalized against the expression level of the housekeeping gene GAPDH. The IDO1 protein expression in tumor tissues from mice treated with phosphate buffer saline solution and DOX were examined by western blotting (C) and immunohistochemistry (D). (E) Protein levels of IDO1 in 4T1-shNC and 4T1-shIDO1 cells detected by western blot.  $\beta$ -actin was used as loading control. (F) Tumor growth in 4T1-shNC and 4T1-shIDO1 tumor bearing BALB/c mice. 4T1-shIDO1 tumor bearing BALB/c mice were injected with DOX at the dosage of 5.0 mg/kg. Data represent means  $\pm$  standard deviation. DOX = doxorubicin; mRNA = messenger RNA; CTLA-4 = cytotoxic T-lymphocyte-associated protein 4; PD-1 = programmed cell death 1; PD-L1 = programmed cell death 1; CSF-1 = cerebrospinal fluid 1; CCL2 = chemokine (C-C motif) ligand 2; IDO1 = indoleamine 2,3-dioxygenase 1; shNC = short hairpin RNA non-target control; shIDO1 = short hairpin RNAs targeting indoleamine 2,3-dioxygenase 1. \* $p < 0.05$ ; † $p < 0.01$ ; ‡ $p < 0.001$ .

### In vitro activities of IDO1-specific inhibitor (NLG919)

Based on the pivotal immune-regulatory role of IDO-1 in the breast tumorigenesis, we detected the *in vitro* effects of the IDO-1 inhibitor NLG919. The chemical structure of NLG919, an imidazole isoindole derivative, is shown in **Figure 3A**. To determine NLG919 activity

against IDO in 4T1 cells, we found that Kyn inhibition rate increases with the increase in NLG919 concentrations added to 4T1 cells (**Figure 3B**).

Previous studies have suggested that IDO-expressing cells can inhibit T-cell proliferation [12]. Thus, we used the cell co-culture system to verify the inhibitory effects of NLG919 on IDO-1. IFN- $\gamma$ -treated 4T1 cells were co-cultured with human CD8<sup>+</sup> T cells in the presence of a soluble anti-CD3 antibody and human recombinant IL-2. We found that NLG919, which led to IDO1 inhibition, significantly promoted T-cell proliferation in the cell co-culture systems in a dose-dependent manner (**Figure 3C**).

### **In vivo anti-tumor effect of DOX, NLG919, and combination of both agents**

As seen in **Figure 4A**, NLG919 and DOX treatment led to significant breast tumor volume suppression in mice both in a time-dependent manner. Notably, in the combinatorial treatment group, NLG919, combined with DOX, exhibited high synergistic antitumor activity. The tumor volumes across the study in this DOX + NLG919 group were maintained at a very low level (**Figure 4A**,  $p < 0.001$ ).

To decipher the potential mechanism of this drug combination, we detected the Kyn/Trp ratios in tumors and plasma by HPLC-MS/MS. The results showed that NLG919 treatment decreased Kyn concentrations in tumors and plasma, whereas DOX levels did not significantly change based on the Kyn concentration. Intriguingly, combined NLG919 and DOX slightly inverted the Kyn concentration in tumors and plasma samples (**Figure 4B**).

Further, PCNA immunohistochemical reactivity within tumors in the control mice with 4T1 cells was the highest among all groups. Lower number of PCNA-positive cells was observed in the DOX and NLG919-only groups in a scattered pattern. Meanwhile, almost no PCNA-

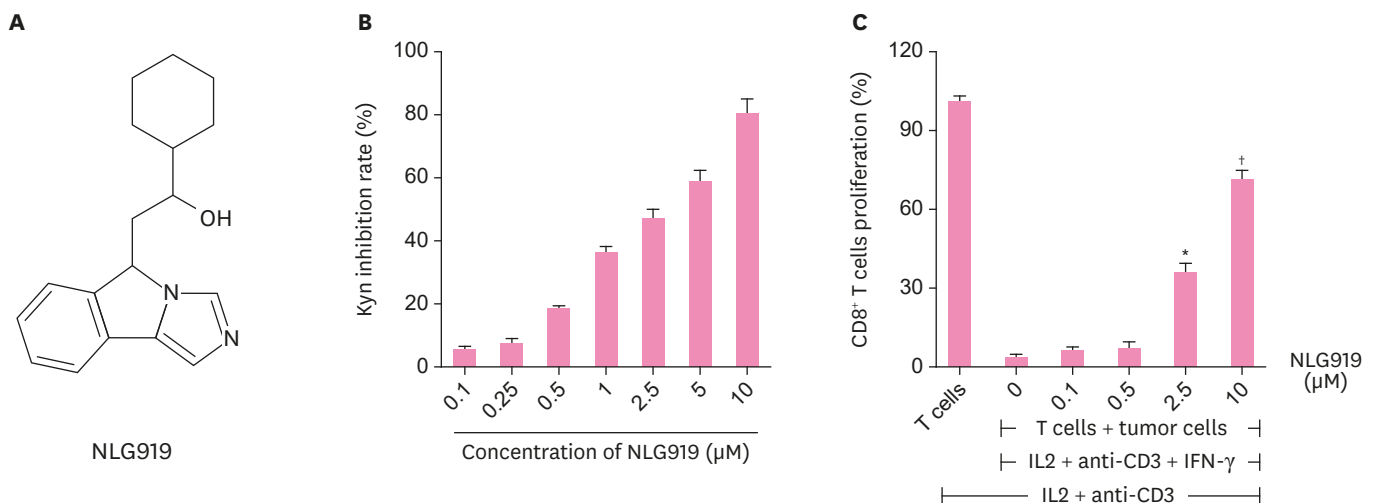


**Figure 3.** *In vitro* activities of IDO1-specific inhibitor (NLG919). (A) Molecular structural formula of NLG919, a highly selective inhibitor of IDO1. (B) NLG919 inhibited IDO1 enzyme activity *in vitro*. The 4T1 cells were treated with IFN- $\gamma$  together with different concentrations of NLG919. Kyn level in supernatant was measured 2 days later using high performance liquid chromatography mass spectrometry. The 4T1 cells treated only with IFN- $\gamma$  were set as blank control. (C) IDO1 inhibition reversed T-cell suppression mediated by IDO-expressing murine breast cancer cells (4T1). The 4T1 cells and splenocytes were co-cultured, and then, treated with IL-2, anti-CD3 antibody, and IFN- $\gamma$  together with NLG919 for 3 days. The proliferation of CD8<sup>+</sup> T cells was examined by fluorescence-activated cell sorting analysis.

Data represent means  $\pm$  standard deviation.

IDO1 = indoleamine 2,3-dioxygenase 1; Kyn = kynurenine; IL = interleukin; IFN = interferon.

\* $p < 0.05$ ; † $p < 0.01$  (versus control).



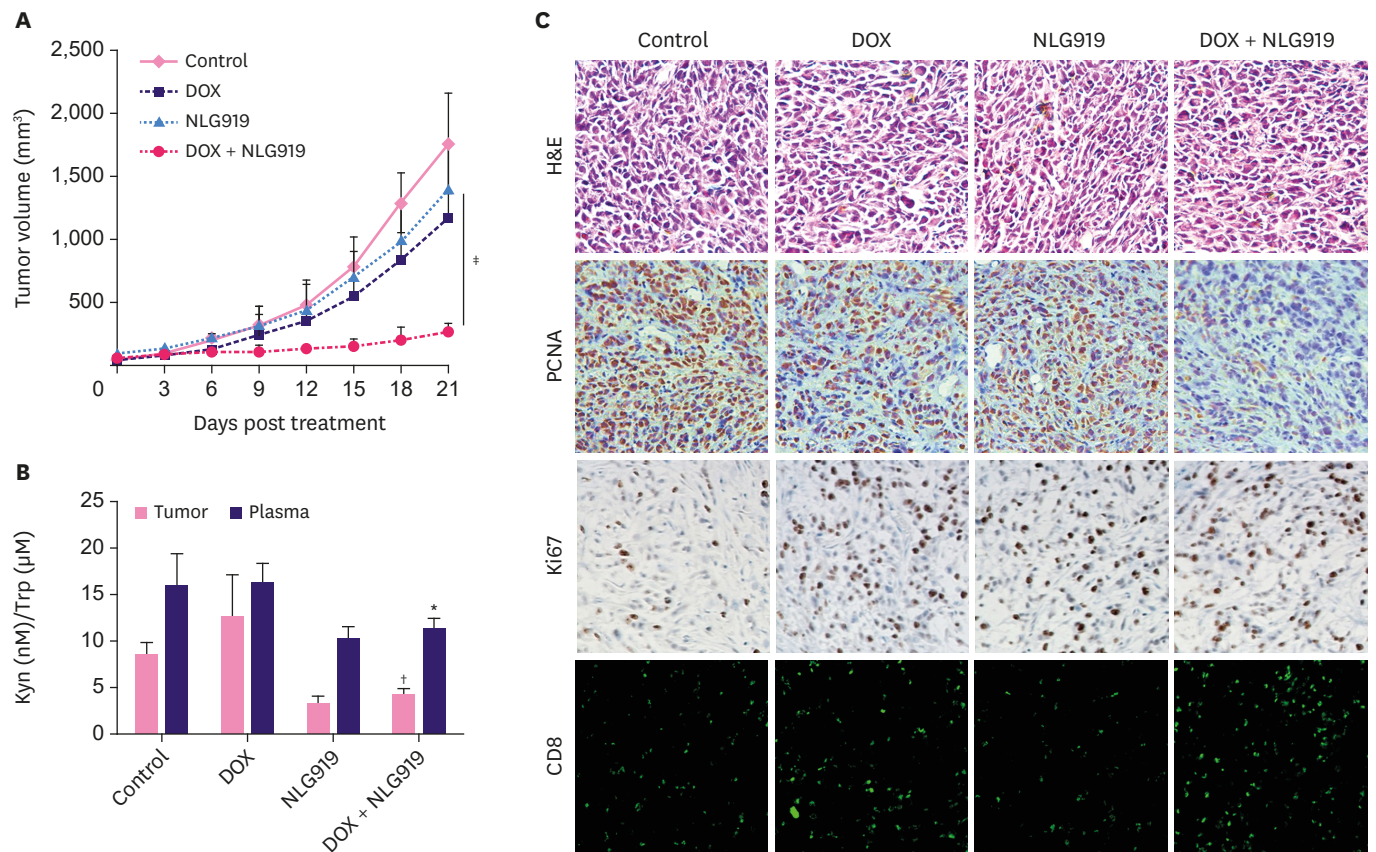


**Figure 4.** *In vivo* anti-tumor effect of DOX, NLG919, and combination of both agents. (A) Inhibition of tumor growth by various treatments in 4T1 tumor-bearing BALB/c mice ( $n = 6$ ). BALB/c mice bearing 4T1 tumors of  $\sim 50 \text{ mm}^3$  volume were treated with either phosphate buffer saline, DOX, NLG919, or a combination of DOX and NLG919 for 5 times after 3 days each; the administration dosage of DOX and NLG919 were 5.0 mg/kg (i.v.) and 20 mg/kg (orally), respectively. (B) NLG919 treatment decreased Kyn levels in tumors and plasma. Kyn/Trp ratios in tumors and plasma were determined by high performance liquid chromatography mass spectrometry at the end of the treatment. (C) H&E, PCNA, and Ki67 staining, and CD8<sup>+</sup> T cells analyses of tumor tissues after treatment with various therapeutic agents. The PCNA-positive proliferating cells and Ki67-positive apoptotic cells are stained brown. CD8<sup>+</sup> T cells are stained green. Data represent means  $\pm$  standard deviation. DOX = doxorubicin; Kyn = kynurenine; Trp = tryptophan; PCNA = proliferating cell nuclear antigen; H&E = hematoxylin and eosin stain. \* $p < 0.05$ ; † $p < 0.01$ ; ‡ $p < 0.001$  (versus DOX group).

positive cells and higher number of Ki67-positive cells were observed in the DOX + NLG919 group (Figure 4C), suggesting DOX + NLG919 could effectively inhibit the cell proliferation and induce cell apoptosis. More importantly, combination therapy significantly promotes the tumor infiltration of CD8<sup>+</sup> cells (Figure 4C).

### Flow cytometry analysis of immune cell subsets and ELISA analysis of cytokine expression in tumor tissues

To explore the possible mechanisms of the combinatorial treatment with NLG919 and DOX, the mature DCs in the total DC populations (CD45, CD11b<sup>+</sup>, CD11c<sup>+</sup>, CD80, and CD86) were analyzed in the tumor cells. From a representative flow cytometry plot and the quantitative analysis results (Figure 5A), we found that DOX + NLG919 group showed a significant increase in the percentage of mature DCs in tumor tissue, compared to all the other 3 groups. The representative plot and quantitative analysis of T-cell population results showed that the DOX + NLG919 group exhibited increase in percentage of CD8<sup>+</sup> T cells in the CD4<sup>+</sup> TIL gated cell populations (Figure 5B,  $p < 0.01$ ). There was only a minor increase in the percentage of CD8<sup>+</sup> T cells in the NLG919 or DOX groups.

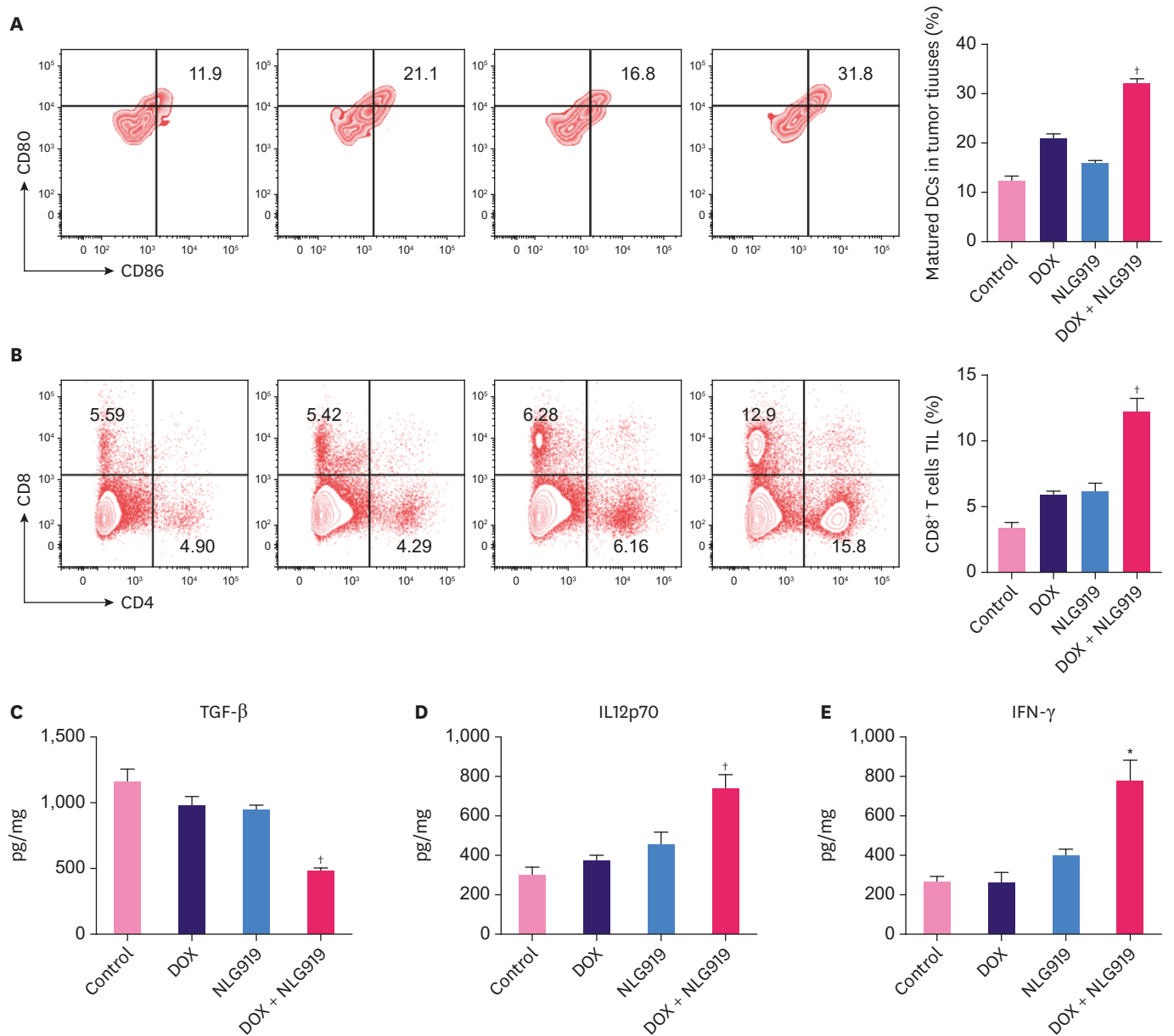


**Figure 5.** Flow cytometry analysis of immune cell subsets and ELISA analysis of cytokine expression in tumor tissues. (A) Flow cytometry gating and histogram analysis of mature DCs in the tumor tissues at the end of treatment. The mature DCs were denoted as CD80<sup>+</sup>CD86<sup>+</sup> populations (gate in CD45<sup>+</sup>CD11b<sup>+</sup>CD11c<sup>+</sup> cell population). (B) Flow cytometry gating and histogram analysis of cytotoxic T cells (CD8<sup>+</sup> T cells) in the CD45<sup>+</sup> TILs in tumor tissues from mice receiving indicated treatment. (C-E) ELISA results of cytokine production in the tumors from mice receiving indicated treatments. Data represent means  $\pm$  standard deviation.

ELISA = enzyme-linked immunosorbent assay; DOX = doxorubicin; DC = dendritic cell; TIL = tumor infiltrating lymphocyte; TGF = transforming growth factor; IL = interleukin; IFN = interferon.

\* $p < 0.05$ ; † $p < 0.01$  (versus DOX group).

The levels of TGF- $\beta$ , IL-12, p70, and IFN- $\gamma$  in supernatants of the tumor tissues were analyzed by ELISA (**Figure 5C-E**), and the results showed that treatment with DOX + NLG919 combination significantly decreased the TGF- $\beta$  level ( $p < 0.01$ ), increased the levels of IL-12p70 ( $p < 0.01$ ) and IFN- $\gamma$  ( $p < 0.05$ ), while the levels of these 3 cytokines remained at the same level in the control, NLG919-only, and DOX-only groups.

## DISCUSSION

DOX is widely considered as one of the most effective chemotherapeutic agents, serving as a first-line drug in different types of cancers [13]. The primary molecular action mechanisms of DOX are associated with DNA replication, which prevents cell proliferation and apoptosis [14]. DOX inserts into DNA strands directly or intercalates into DNA strands by modulating replication-associated enzymes [15]. The anti-tumor activity of DOX is also associated with reactive oxygen species generation in the cells [16]. In this study, we first demonstrated that clinically used anthracycline DOX can induce immunogenic death in 4T1 murine triple-negative breast cancer cells, indicated by CRT exposure and increased ATP and HMGB1 release.

Intriguingly, we found DOX treatment on breast tumor cells induced upregulation of IDO1. These results revealed other potential mechanisms of DOX action on tumor repression, especially in MBC, on which the conventional DOX treatment exhibits various adverse effects and subsequent therapeutic failure [17]. Tumor cells treated with DOX can exert a "vaccine" function, activate the body's immune system, and prevent tumor recurrence. Several studies have shown that IDO1 can catalyze the metabolism of Trp in the tumor microenvironment, resulting in decrease in Trp levels, which, in turn, interferes with the function of cytotoxic cells, leading to immunosuppression [9,18-20]. The immune system is critical in modulating cancer progression, and immune checkpoint therapies have been used for clinical treatment of cancer, targeting regulatory pathways that affect T cells to enhance antitumor immune responses [21]. Among all investigational immune checkpoint targets, IDO has been reported to increase the Kyn secretion to inhibit effector T cells, thus promoting immune escape and tumor progression in various human cancers [22]. Expression level of IDO1 was high in a number of tumor samples. For instance, IDO1 showed a significantly higher mRNA and protein expression levels in cervical cancer than in normal cervix, as well as other cancer tissues [23]. High expression of IDO was observed in oral squamous cell carcinoma (OSCC), representing a significant negative prognostic factor in OSCC patients [24]. It has been demonstrated that high intratumoral IDO1 mRNA levels correlate with a poor glioblastoma patient prognosis, and the increased IDO1 levels are associated with human-infiltrating T cells [25]. In our study, we found that the expression of IDO in breast cancer tumor tissues was significantly increased after DOX treatment.

IDO inhibitors have been reported to improve responses during cancer chemotherapy, but are only scarcely efficacious when used as a single agent [26]. Using mammary tumor virus-neu mice based breast cancer model, a previous study showed that small-molecule inhibitors of IDO acted synergistically with cytotoxic agents to elicit regression of established tumors refractory to single-agent therapy [27]. Some recent progress in understanding the immunological changes associated with chemotherapy, and advances in combining checkpoint blockade agents, including IDO inhibitor, with conventional chemotherapy is promising for a growing number of cancers [28]. NLG919, which was developed by NewLink and later licensed by Genentech, is a potent IDO pathway inhibitor with desirable pharmacological properties for the treatment of immunosuppression associated with cancer [29]. We first measured the *in vitro* activity of NLG919 by measuring the IDO1 enzyme activity, and our results showed that NLG919 activity enhanced the Kyn inhibition rate in a dose-dependent manner. In addition, CD8<sup>+</sup> T cell proliferation assay results showed that IDO1 inhibition reversed T-cell suppression mediated by IDO-expressing 4T1 murine breast cancer cells.

To further explore whether the administration of specific small molecule inhibitor, NLG919, combined with DOX, can achieve better treatment effects for breast cancer, we constructed a 4T1 murine breast tumor model and subjected it to either the DOX, NLG919, or the combination therapy. The results showed that DOX and NLG919 alone can only slightly restrict the growth rate of the tumor, while the combination treatment significantly inhibited the tumor growth, indicating that the 2 drugs exhibited synergistic effect. Flow cytometry analysis of the infiltration of tumor tissue revealed that the proportion of activated DCs and cytotoxic sputum cells in the combined treatment group was significantly higher than that of the control group and the treatment group alone. At the same time, the expression levels of immunosuppressive cytokines (such as TGF- $\beta$ ) in combination therapy are relatively low, while the expression levels of cytokines (such as IL-12p70 and IFN- $\gamma$ ) associated with immune activation and tumor elimination are significantly upregulated. Although several studies have utilized a variety of human breast cancer cells, we selected 4T1 cells to establish the animal model. Since the tumor growth and metastatic spread of 4T1 cells in BALB/c mice could mimic human breast cancer very closely, it is an ideal type of cell to be used in our study that involved non-surgical engrafting. In summary, chemotherapeutic drug, DOX, that induced cellular immunogenic death can act synergistically with IDO1 inhibitors, killing tumor cells and effectively activating the body's anti-tumor response. Owing to the better tumor treatment effects, such combination therapy is a promising breast cancer treatment strategy. Although we observed anti-tumor effects of the combined treatment strategy in breast cancer animal model, the underlying molecular mechanism of this strategy needs to be further explored. In addition, the clinical validation of DOX and NLG919 is essential to verify the side effects of these 2 agents.

In summary, this study indicated that the small molecule inhibitor NLG919 enhanced the antitumor efficacy of DOX in 4T1 murine breast tumor model, indicating the combination of chemotherapeutic agent with IDO inhibitor-based immunotherapeutic agent as a new promising strategy for the treatment of breast cancer.

## SUPPLEMENTARY MATERIALS

### Supplementary Figure 1

Cell viability of 4T1 cells after treated with different concentration of DOX for 24 hours. The half-maximal inhibitory concentration value can be calculated according to cell viabilities.

[Click here to view](#)

### Supplementary Figure 2

(A) Protein levels of IDO1 in DOX-treated 4T1-shNC and 4T1-shIDO1 were detected by western blot.  $\beta$ -actin was detected as control. (B) Cell viability after DOX and IDO1 plasmid (or GFP plasmid) for 24 hours, the concentration of DOX was 0.25  $\mu$ M.

[Click here to view](#)

## REFERENCES

1. Hutchinson L. Breast cancer: challenges, controversies, breakthroughs. *Nat Rev Clin Oncol* 2010;7:669-70.  
[PUBMED](#) | [CROSSREF](#)

2. Siegel RL, Miller KD, Jemal A. Cancer Statistics, 2017. *CA Cancer J Clin* 2017;67:7-30.  
[PUBMED](#) | [CROSSREF](#)
3. Anampa J, Makower D, Sparano JA. Progress in adjuvant chemotherapy for breast cancer: an overview. *BMC Med* 2015;13:195.  
[PUBMED](#) | [CROSSREF](#)
4. Sledge GW, Mamounas EP, Hortobagyi GN, Burstein HJ, Goodwin PJ, Wolff AC. Past, present, and future challenges in breast cancer treatment. *J Clin Oncol* 2014;32:1979-86.  
[PUBMED](#) | [CROSSREF](#)
5. Garg AD, More S, Rufo N, Mece O, Sassano ML, Agostinis P, et al. Trial watch: Immunogenic cell death induction by anticancer chemotherapeutics. *OncoImmunology* 2017;6:e1386829.  
[PUBMED](#) | [CROSSREF](#)
6. Kroemer G, Galluzzi L, Kepp O, Zitvogel L. Immunogenic cell death in cancer therapy. *Annu Rev Immunol* 2013;31:51-72.  
[PUBMED](#) | [CROSSREF](#)
7. Binnewies M, Roberts EW, Kersten K, Chan V, Fearon DF, Merad M, et al. Understanding the tumor immune microenvironment (TIME) for effective therapy. *Nat Med* 2018;24:541-50.  
[PUBMED](#) | [CROSSREF](#)
8. Lu J, Liu X, Liao YP, Salazar F, Sun B, Jiang W, et al. Nano-enabled pancreas cancer immunotherapy using immunogenic cell death and reversing immunosuppression. *Nat Commun* 2017;8:1811.  
[PUBMED](#) | [CROSSREF](#)
9. Moon YW, Hajjar J, Hwu P, Naing A. Targeting the indoleamine 2,3-dioxygenase pathway in cancer. *J Immunother Cancer* 2015;3:51.  
[PUBMED](#) | [CROSSREF](#)
10. Chen X, Parelkar SS, Henchey E, Schneider S, Emrick T. PolyMPC-doxorubicin prodrugs. *Bioconjug Chem* 2012;23:1753-63.  
[PUBMED](#) | [CROSSREF](#)
11. Yue EW, Douty B, Wayland B, Bower M, Liu X, Leffet L, et al. Discovery of potent competitive inhibitors of indoleamine 2,3-dioxygenase with *in vivo* pharmacodynamic activity and efficacy in a mouse melanoma model. *J Med Chem* 2009;52:7364-7.  
[PUBMED](#) | [CROSSREF](#)
12. Munn DH, Shafizadeh E, Attwood JT, Bondarev I, Pashine A, Mellor AL. Inhibition of T cell proliferation by macrophage tryptophan catabolism. *J Exp Med* 1999;189:1363-72.  
[PUBMED](#) | [CROSSREF](#)
13. Tacar O, Sriamornsak P, Dass CR. Doxorubicin: an update on anticancer molecular action, toxicity and novel drug delivery systems. *J Pharm Pharmacol* 2013;65:157-70.  
[PUBMED](#) | [CROSSREF](#)
14. Müller I, Jenner A, Bruchelt G, Niethammer D, Halliwell B. Effect of concentration on the cytotoxic mechanism of doxorubicin--apoptosis and oxidative DNA damage. *Biochem Biophys Res Commun* 1997;230:254-7.  
[PUBMED](#) | [CROSSREF](#)
15. Dickey JS, Rao VA. Current and proposed biomarkers of anthracycline cardiotoxicity in cancer: emerging opportunities in oxidative damage and autophagy. *Curr Mol Med* 2012;12:763-71.  
[PUBMED](#) | [CROSSREF](#)
16. Mizutani H, Tada-Oikawa S, Hiraku Y, Kojima M, Kawanishi S. Mechanism of apoptosis induced by doxorubicin through the generation of hydrogen peroxide. *Life Sci* 2005;76:1439-53.  
[PUBMED](#) | [CROSSREF](#)
17. Rosch JG, Brown AL, DuRoss AN, DuRoss EL, Sahay G, Sun C. Nanoalginates via inverse-micelle synthesis: doxorubicin-encapsulation and breast cancer cytotoxicity. *Nanoscale Res Lett* 2018;13:350.  
[PUBMED](#) | [CROSSREF](#)
18. Munn DH, Mellor AL. IDO in the tumor microenvironment: inflammation, counter-regulation, and tolerance. *Trends Immunol* 2016;37:193-207.  
[PUBMED](#) | [CROSSREF](#)
19. Löb S, Königsrainer A, Rammensee HG, Opelz G, Terness P. Inhibitors of indoleamine-2,3-dioxygenase for cancer therapy: can we see the wood for the trees? *Nat Rev Cancer* 2009;9:445-52.  
[PUBMED](#) | [CROSSREF](#)
20. Prendergast GC, Malachowski WP, DuHadaway JB, Muller AJ. Discovery of IDO1 inhibitors: from bench to bedside. *Cancer Res* 2017;77:6795-811.  
[PUBMED](#) | [CROSSREF](#)
21. Sharma P, Allison JP. The future of immune checkpoint therapy. *Science* 2015;348:56-61.  
[PUBMED](#) | [CROSSREF](#)



22. Selvan SR, Dowling JP, Kelly WK, Lin J. Indoleamine 2,3-dioxygenase (IDO): biology and target in cancer immunotherapies. *Curr Cancer Drug Targets* 2016;16:755-64.  
[PUBMED](#) | [CROSSREF](#)
23. Qin Y, Ekmekcioglu S, Forget MA, Szekvolgyi L, Hwu P, Grimm EA, et al. Cervical cancer neoantigen landscape and immune activity is associated with human papillomavirus master regulators. *Front Immunol* 2017;8:689.  
[PUBMED](#) | [CROSSREF](#)
24. Laimer K, Troester B, Kloss F, Schafer G, Obrist P, Perathoner A, et al. Expression and prognostic impact of indoleamine 2,3-dioxygenase in oral squamous cell carcinomas. *Oral Oncol* 2011;47:352-7.  
[PUBMED](#) | [CROSSREF](#)
25. Zhai L, Ladomersky E, Lauing KL, Wu M, Genet M, Gritsina G, et al. Infiltrating T Cells increase IDO1 expression in glioblastoma and contribute to decreased patient survival. *Clin Cancer Res* 2017;23:6650-60.  
[PUBMED](#) | [CROSSREF](#)
26. Uyttenhove C, Pilotte L, Théate I, Stroobant V, Colau D, Parmentier N, et al. Evidence for a tumoral immune resistance mechanism based on tryptophan degradation by indoleamine 2,3-dioxygenase. *Nat Med* 2003;9:1269-74.  
[PUBMED](#) | [CROSSREF](#)
27. Muller AJ, DuHadaway JB, Donover PS, Sutanto-Ward E, Prendergast GC. Inhibition of indoleamine 2,3-dioxygenase, an immunoregulatory target of the cancer suppression gene Bin1, potentiates cancer chemotherapy. *Nat Med* 2005;11:312-9.  
[PUBMED](#) | [CROSSREF](#)
28. Cook AM, Lesterhuis WJ, Nowak AK, Lake RA. Chemotherapy and immunotherapy: mapping the road ahead. *Curr Opin Immunol* 2016;39:23-9.  
[PUBMED](#) | [CROSSREF](#)
29. Meng X, Du G, Ye L, Sun S, Liu Q, Wang H, et al. Combinatorial antitumor effects of indoleamine 2,3-dioxygenase inhibitor NLG919 and paclitaxel in a murine B16-F10 melanoma model. *Int J Immunopathol Pharmacol* 2017;30:215-26.  
[PUBMED](#) | [CROSSREF](#)